Synthesis of [11C]uric acid, using [11C]phosgene, as a possible biomarker in PET imaging for diagnosis of gout

doi: 10.1016/j.bmcl.2011.11.055

Synthesis of [^{11}C]uric acid, using [^{11}C]phosgene, as a possible biomarker in PET imaging for diagnosis of gout

Keiji Yashio[a*], Yumiko Katayama[a], Tadayuki Takashima[a], Naoki Ishiguro[b], Hisashi Doi[a], Masaaki Suzuki[a], Yasuhiro Wada[a], Ikumi Tamai[c] and Yasuyoshi Watanabe[a*]

k.yashio@riken.jp (K. Yashio)

ykatayama@riken.jp (Y. Katayama)

ttakashima@riken.jp (T. Takashima)

naoki.ishiguro@boehringer-ingelheim.com (N. Ishiguro)

hisashi.doi@riken.jp (H. Doi)

suzuki.masaaki@riken.jp (M. Suzuki)

yasuwada@riken.jp (Y. Wada)

tamai@p.kanazawa-u.ac.jp (I. Tamai)

yywata@riken.jp (Y. Watanabe)

[a]RIKEN Center for Molecular Imaging Science (CMIS), 6-7-3 Minatojima-minamimachi, Chuo-ku, Kobe, Hyogo 650-0047, Japan

[b]Department of Pharmacokinetics and Non-Clinical Safety, Kobe Pharma Research Institute, Nippon Boehringer Ingelheim Co. Ltd.

[c]Department of Membrane Transport and Biopharmaceutics, Faculty of Pharmacy, Institute of Medical, Pharmaceutical and Health Sciences, Kanazawa University

***Corresponding author**: Keiji Yashio

Molecular Probe Dynamics Laboratory, RIKEN Center for Molecular Imaging Science

6-7-3 Minatojima-minamimachi, Chuo-ku, Kobe, Hyogo 650-0047, Japan

Phone: +81-78-304-7124; Fax: +81-78-304-7126; E-mail: k.yashio@riken.jp (K. Yashio)

Keywords: [^{11}C]uric acid, Positron Emission Tomography (PET), [^{11}C]phosgene, hyperuricemia, gout

Abstract

The synthesis and *in vivo* evaluation of ^{11}C-labeled uric acid ([^{11}C]**1**), a potential imaging agent for the diagnosis of urate-related life-style diseases, was performed using positron emission tomography (PET) image analysis. First, the synthesis of [^{11}C]**1** was achieved by reacting 5,6-diaminouracil (**2**) with ^{11}C-labeled phosgene ([^{11}C]$COCl_2$). The radiochemical yield of [^{11}C]**1** was 37±7% (decay-corrected based on [^{11}C]$COCl_2$) with specific radioactivities of 96-152 GBq/μmol at the end of synthesis (n = 6). The average time of radiosynthesis from the end of bombardment, including formulation, was about 30 min with >98% radiochemical purity. Second, the synthetic approach to [^{11}C]**1** was optimized using 5,6-diaminouracil sulfate (**3**) with [^{11}C]$COCl_2$ in the presence of 1,8-bis(dimethylamino)naphthalene. [^{11}C]**1** was synthesized in 36±6% radiochemical yield, 89-142 GBq/μmol of specific radioactivities, and 98% radiochemical purity by this method (n = 5). This allowed the synthesis of [^{11}C]**1** to be carried out repeatedly and the radiochemical yield, specific radioactivities, average time of synthesis, and radiochemical purity of [^{11}C]**1** were similar to those obtained using **2**. PET studies in rats showed large differences in the accumulation of radioligand in the limbs under normal and hyperuricemic conditions. Thus, an efficient and convenient automated synthesis of [^{11}C]**1** has been developed, and preliminary PET evaluation of [^{11}C]**1** confirmed the increased accumulation of radioactivity in the limbs of a rat model of hyperuricemia.

Abbreviations

PET: Positron Emission Tomography

DMPU: *N*,*N*'-dimethylpropyleneurea

DIPEA: *N*,*N*-diisopropylethylamine

High serum uric acid level, or hyperuricemia, is a hallmark of gout, and lead to the crystallization of monosodium urate in joints and the formation of urinary tract calculi. In hyperuricemia, approximately 80% of patients also suffer from some type of lifestyle-related disease such as hypertension, cardiovascular disease, obesity and dyslipidemia; however, the clinical significance of these conditions remains controversial [1]. Baseline laboratory tests for gout include urinalysis, serum uric acid measurements and other biochemical examinations of blood. Although hyperuricemia is a risk factor for the development of gout and other disorders, the relationship between serum uric acid levels and the pathogenesis of these disorders remains unclear. Other diagnostic methods for gout include the examination of the presence of polymorphonuclear leukocytes and intracellular monosodium urate crystals in synovial fluid aspirated from an inflamed joint, but other disorders can sometimes mimic gout. Thus, measurement of tissue concentrations of uric acid is essential for the early diagnosis of gout and other urate-related life-style diseases.

Positron emission tomography (PET) is a molecular and functional imaging technique that allows highly sensitive, noninvasive, quantitative and repetitive visualization of biological functions in living animals *in vivo* with biologically active compounds labeled with short-lived positron emitting radionuclides (^{11}C, ^{13}N, ^{15}O and ^{18}F) that do not affect the biochemical and physiochemical characteristics [2-8]. Generally, the tracer doses used in PET studies are very small, typically less than 1/100 of the actual pharmacological dose or 100

μg/dose [9]. Thus, PET has recently been applied to human microdose studies at early stages of drug and biomarker development [10]. The development of a quantitative PET imaging method with radiolabeled uric acid would enable the noninvasive assessment of uric acid accumulation in diseased tissue and may also demonstrate the feasibility of PET imaging analysis for the early diagnosis of gout and relevant diseases.

In vivo molecular imaging with small animal models bridges the gap between laboratory research and human clinical studies. In rodents, uric acid is the product of purine metabolism, and is subsequently degraded by the hepatic enzyme uricase into a water-soluble product (allantoin) [11]. In humans, uric acid is the end product of purine metabolism due to the lack of uricase [12,13]. Several groups have reported that hyperuricemia can be induced in rats by administering the uricase inhibitor oxonic acid [14]. Oxonic acid-treated rats can therefore serve as a useful animal model for investigating the pathogenesis of gout, as well as a number of other uric acid-related disorders.

Herein, we report the first synthesis of ^{11}C-labeled uric acid ([^{11}C]**1**, Fig. 1) using [^{11}C]$COCl_2$. Subsequently, we compared the accumulation of the radioligand in the tissues of hyperuricemic rats with that in normal rats by small-animal PET using [^{11}C]**1**.

The synthesis of PET molecular probes labeled with short-lived radionuclides requires a very rapid and simple labeling process. We selected ^{11}C-labeled phosgene ([^{11}C]$COCl_2$) as a labeling agent for synthesis of [^{11}C]**1**. [^{11}C]$COCl_2$ is highly reactive for the

introduction of a [^{11}C]carbonyl group and is very useful for synthesis of heterocyclic compounds [15-17]. This approach involves efficient construction of cyclic [^{11}C]urea moiety, which requires reliable preparation of [^{11}C]$COCl_2$ and uses 5,6-diaminouracil (**2**) as a starting material (Scheme 1).

Thus, **2** was reacted with [^{11}C]$COCl_2$ to give [^{11}C]**1** in *N*,*N*'-dimethylpropyleneurea (DMPU) solution at 100°C for 2 min. [^{11}C]$COCl_2$ was synthesized from [^{11}C]methane via [^{11}C]CCl_4 according to a previously reported method [18,19]. [^{11}C]Methane was produced using a CYPRIS HM-12S cyclotron (Sumitomo Heavy Industries) by the $^{14}N(p,\alpha)^{11}C$ nuclear reaction in N_2 containing H_2 (10%) on an aluminum target. Bombardment was carried out with a 30 μA beam of 12 MeV protons for 10 min. The [^{11}C]methane and Cl_2 gas mixture was passed through a quartz U-tube at 560°C to give [^{11}C]CCl_4. The [^{11}C]CCl_4 was next passed through the oxidation tube of a Kitagawa gas detection tube system at room temperature at a flow rate of 50 mL/min to afford [^{11}C]$COCl_2$. The [^{11}C]$COCl_2$ was bubbled into a DMPU solution [20] (150 μL) containing **2** (1.0 mg, 7.04 μmol) and *N*,*N*-diisopropylethylamine (DIPEA) [21] (9.10 mg, 70.4 μmol) at -10°C for 2 min. The mixture was then heated at 100°C for 2 min to form [^{11}C]**1**. After cooling, the reaction mixture was diluted with phosphate buffer and injected into a preparative HPLC system for purification of [^{11}C]**1** (column: Unison UK-C18, 7 mm, Imtakt, 10 × 250 mm ; solvents and conditions: 10 mM Phosphate Buffer (pH 2.5), 4 mL/min, t_R [^{11}C]**1**: 11.5–12.0 min). The purified fraction was diluted about

10-fold with saline prior to the injection. The yield of [^{11}C]**1** was 1314 ± 226 MBq at the end of synthesis (n = 6) (Scheme 1). The decay corrected radiochemical yield of [^{11}C]**1** was 37±7% based on [^{11}C]$COCl_2$ [22]. The overall radiosynthesis time was ca. 30 min from the end of bombardment.

The synthesized [^{11}C]**1** was identified by co-chromatography with authentic uric acid and found to be radiochemically homogeneous by HPLC. Figure 2 shows HPLC chromatograms before and after purification. These chromatograms show that [^{11}C]**1** was produced as the major radioactive peak in the reaction mixture (Fig. 2A), and the radiochemical purity of [^{11}C]**1** was ca. 98% after purification (Fig. 2B). The specific activity of [^{11}C]**1** was 96-152 GBq/μmol at the end of synthesis. Although the synthesis of [^{11}C]**1** from **2** was successful with high RI, and chemical yield was sufficient for use a PET molecular probe, there are some practical disadvantages in using **2**, such as its high cost, difficulty in handling and its chemical instability for long-term storage.

In order to overcome these problems, synthesis was modified, using 5,6-diaminouracil sulfate (**3**) as a starting material (Scheme 2), which is commercially available at lower cost and is easier to handle than **2**. As **3** did not react with [^{11}C]$COCl_2$ without neutralization, appropriate labeling conditions were investigated using several bases for the neutralization *in situ* of **3** in labeling reaction (Table 1). It was shown that, trialkylamines were unsuccessful (entries 1 and 2), and *t*-BuOK and $KN(SiMe_3)_2$ were also

found to be ineffective in this reaction (entries 3 and 5). On the other hand, a small amount of [^{11}C]**1** was obtained when 18-crown-6 was added to improve reactivity of $KN(SiMe_3)_2$ (entry 6), but had no effect in the case of *t*-BuOK (entry 4). Next, we investigated the use of the highly basic but very weakly nucleophilic (non-nucleophilic proton trapping) bases 1,8-bis(dimethylamino)naphthalene and 1,8-bis(*N*,*N*,*N*',*N*'-tetramethylguanidino)naphthalene, which are well-known proton sponges (entries 7 and 8). [^{11}C]**1** was synthesized in 36±6% radiochemical yield, 89-142 GBq/μmol of specific radioactivities, and 98% radiochemical purity (entry 7, n = 5). The labeling reaction with proton sponge was conducted under the same conditions [23] as used previously with **2**, and [^{11}C]**1** was reproducibly obtained with similar yield and specific radioactivities as obtained with **2**. Based on this experimental data, it is clear that a proton sponge is effective in this labeling reaction using **3**.

Subsequently, we performed PET studies for [^{11}C]**1** in anesthetized rats [24-27] under normal or hyperuricemic conditions, in which rats were premedicated with potassium oxonate (250 mg/kg, i.p.) [11,14]. After intravenous bolus injection of [^{11}C]**1** (22-30 MBq per animal) via the tail vein, whole body scans were performed with 180-s duration for 1 bed pass, in addition to blood sampling via the femoral vein. Data were sorted into dynamic sinograms for each bed pass. Emission data were reconstructed by Fourier Rebinning and maximum likelihood expectation maximization. Regions of interest (ROIs) were delineated for the limbs, which were visually identifiable, using the Pmod ver. 3.0 program (PMOD Technologies Ltd.,

Zurich, Switzerland). Radioactivity in the ROIs was estimated by percent of total radioactivity at each frame.

The maximum intensity projection PET images in the whole body following administration of [^{11}C]**1** to rats under normal or hyperuricemic conditions are shown in Fig. 3. The radioactivity was mainly eliminated via renal excretion in both rats. The radioactivity in the limbs was clearly identifiable under hyperuricemic conditions, as compared with normal conditions. The distribution of radioactivity in the limbs under hyperuricemic conditions was 2.6-fold higher than that under normal conditions (Fig. 4A). On the other hand, the radioactivity in the blood at 60 min (Fig. 4B) and that remained in the whole body at 65-70 min following administration of [^{11}C]1 (Fig. 4C), in which the radioactivity excreted via renal excretion was excluded, were 1.6-fold and 1.5-fold higher under hyperuricemic conditions than under normal conditions, respectively, but the difference did not reach the statistical significance. Endogenous uric acid level in plasma under hyperuricemic conditions was 12.7-fold higher than that under normal conditions (Fig. 4D). Representative radio-chromatograms of blood specimens showed that most of the radioactivity in the blood was derived from the soluble metabolite ([^{11}C]allantoin) under normal conditions, whereas almost 100% of the radioactivity was present as the parent [^{11}C]**1** under hyperuricemic conditions (Fig. 5).

The ratios of total radioactivity in the blood under hyperuricemic and normal conditions (1.6-fold) are lower than those for the distribution of radioactivity in the limbs (2.6-fold). The radioactivity derived from [^{11}C]**1** in blood under hyperuricemic conditions, as calculated by radiometabolite analysis, was 0.57±0.16% of the injected dose, whereas that under normal conditions was below the limit of detection. On the other hand, the ratios of endogenous uric acid levels in plasma under hyperuricemic and normal conditions (12.7-fold) were much higher than those for the distribution of radioactivity in the limbs. These results suggest that the radioactivity of [^{11}C]**1** accumulates in areas of low temperature such as joints, which can be difficult to determine by analysis of blood uric acid levels and endogenous uric acid levels in plasma. The overall transport mechanism of [^{11}C]**1** between blood and the joint region has been unknown, but it has been reported that uric acid is a substrate for GLUT9 (SLC2A9), which is expressed in chondrocytes [28]. The uptake of [^{11}C]**1** into the joint may also provide the information about the function of GLUT9 in chondrocytes.

The present PET studies in rats with [^{11}C]**1** clearly suggest the feasibility of clinical diagnosis of gout and the accumulation of urate in joints. As the PET image analysis with [^{11}C]**1** focus on the tissue distribution and renal excretion of uric acid, but not the production of uric acid, it is also possible that PET study with [^{11}C]**1** is useful for the in vivo evaluation of the impact of variations in excretion in the gastrointestinal tract and the renal excretion of

uric acid. This may be confirmed using quantitative PET image analysis of the abdominal area in future studies.

In conclusion, an efficient repeatable, convenient and automated synthesis method for [^{11}C]uric acid has been developed. Preliminary PET evaluation of [^{11}C]uric acid was performed in a rat model of hyperuricemia, and clearly showed the potential of [^{11}C]uric acid as a PET molecular probe for the diagnosis of hyperuricemia, gout and other urate-related life-style diseases, and for development of anti-gout drugs with better outcome and less adverse effects.

Acknowledgments

We would like to thank Mr. Masahiro Kurahashi (Sumitomo Heavy Industries Accelerator Service Ltd.) for operating the cyclotron. We are also grateful to Ms. Emi Hayashinaka of the RIKEN Center for Molecular Imaging Science, Ms. Naoko Otsu, Mr. Masahito Takatani, and Dr. Wataru Kishimoto of Nippon Boehringer Ingelheim for their expert technical assistance and supervision of this study.

References

1. Vaccarino, V.; Krumholz, H. M. *Ann Intern Med* **1999,** *131*, 62.

2. Willmann, J. K.; van Bruggen, N.; Dinkelborg, L. M.; Gambhir, S. S. *Nat Rev Drug Discov* **2008,** *7*, 591.

3. Riemann, B.; Schafers, K. P.; Schober, O.; Schafers, M. *Q J Nucl Med Mol Imaging* **2008,** *52*, 215.

4. Bergström, M.; Grahnen, A.; Långström, B. *Eur J Clin Pharmacol* **2003,** *59*, 357.

5. Miller, P. W.; Long, N. J.; Vilar, R.; Gee, A. D. *Angew Chem Int Ed Engl* **2008,** *47*, 8998.

6. Fowler, J. S.; Wolf, A. P. *Acc. Chem. Res.* **1997,** *30*, 181.

7. Phelps, M. E. *PET: Molecular Imaging and its Biological Applications*; New York: Springer-Verlag, 2004.

8. Ametamey, S. M.; Honer, M.; Schubiger, P. A. *Chem Rev* **2008,** *108*, 1501.

9. Bergström, M.; Hargreaves, R. J.; Burns, H. D.; Goldberg, M. R.; Sciberras, D.; Reines, S. A.; Petty, K. J.; Ögren, M.; Antoni, G.; Långström, B.; Eskola, O.; Scheinin, M.; Solin, O.; Majumdar, A. K.; Constanzer, M. L.; Battisti, W. P.; Bradstreet, T. E.; Gargano, C.; Hietala, J. *Biol Psychiatry* **2004,** *55*, 1007.

10. Lappin, G.; Garner, R. C. *Nat Rev Drug Discov* **2003,** *2*, 233.

11. Johnson, W. J.; Stavric, B.; Chartrand, A. *Proc Soc Exp Biol Med* **1969,** *131*, 8.

12. Wu, X. W.; Muzny, D. M.; Lee, C. C.; Caskey, C. T. *J Mol Evol* **1992,** *34*, 78.

13. Conger, J. D.; Falk, S. A.; Guggenheim, S. J.; Burke, T. J. *J Clin Invest* **1976,** *58*, 681.

14. Yonetani, Y.; Ishii, M.; Iwaki, K. *Jpn J Pharmacol* **1980,** *30*, 829.

15. Vander Borght, T.; Labar, D.; Pauwels, S.; Lambotte, L. *Int J Rad Appl Instrum A* **1991,** *42*, 103.

16. Steel, C. J.; Brady, F.; Luthra, S. K.; Brown, G.; Khan, I.; Poole, K. G.; Sergis, A.; Jones, T.; Price, P. M. *Appl Radiat Isot* **1999,** *51*, 377.

17. Roeda, D.; Dolle, F. *Curr Top Med Chem* **2010,** *10*, 1680.

18. Nishijima, K.; Kuge, Y.; Seki, K.; Ohkura, K.; Motoki, N.; Nagatsu, K.; Tanaka, A.; Tsukamoto, E.; Tamaki, N. *Nucl Med Biol* **2002,** *29*, 345.

19. Ogawa, M.; Takada, Y.; Suzuki, H.; Nemoto, K.; Fukumura, T. *Nucl Med Biol* **2010,** *37*, 73.

20. **2** is insoluble many organic solvents (ether, THF, chloroform, dichloromethane, toluene, etc…), and doesn't react with [^{11}C]$COCl_2$ in these solvents. Then preheating (100 °C, 5 min) of **2** in DMPU is necessary for the solubilization before labeling reaction.

21. The labeling reaction can carry out without the base, but the yield of [^{11}C]**1** decrease.

22. The yield of [^{11}C]**1** was determined based on [^{11}C]$COCl_2$. The yield of [^{11}C]$COCl_2$ is about 5500 MBq (EOS) based on the yield of [^{11}C]*N,N'*-diphenylurea.

23. The preheating (100 °C, 5 min) is necessary for the solubilization and the neutralization before labeling reaction. The synthesized [^{11}C]$COCl_2$ was bubbling through at -10 °C in a reaction vessel containing **3** (1.7 mg, 7.09 μmol) and 1,8-bis(dimethylamino)naphthalene (9.1 mg, 42.5 μmol) dissolved in 150 μL of DMPU for 2 min. After that, the mixture was heated at 100 °C for 2 min. Next, the reaction mixture was diluted with phosphate buffer and injected to a preparative HPLC system, and purified [^{11}C]**1** was available.

24. PET scans on male Sprague-Dawlay (SD) rats using a MicroPET Focus220 scanner (Siemens Co., Ltd, Knoxville, TN, USA). Rats cannulated into the femoral vein were anesthetized with isoflurane.

25. Yamashita, S.; Takashima, T.; Kataoka, M.; Oh, H.; Sakuma, S.; Takahashi, M.; Suzuki, N.; Hayashinaka, E.; Wada, Y.; Cui, Y.; Watanabe, Y. *J Nucl Med* **2011,** *52*, 249.

26. The amount of radioactivity associated with each intact radiotracer and its metabolite was calculated as a percentage of the total amount radioactivity.

27. The blood radioactivity was measured using a 1470 WIZARD® Automatic Gamma Counter (PerkinElmer, Waltham, MA, USA). To compare the composition of the radioactivity in blood, radio-metabolite analysis of the blood specimen was performed using

HPLC system (Shimadzu, Kyoto, Japan) with a coupled NaI(Tl) positron detector UG–SCA30 (Universal Giken, Kanagawa, Japan).

28, So A, Thorens B.. *J Clin Invest.* **2010,** 120:1791.

Figure 1. Chemical structure of uric acid and [^{11}C]**1**.

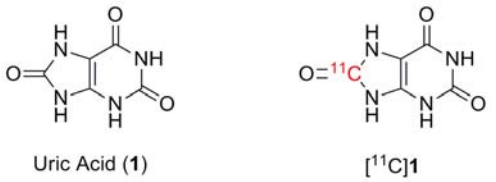

Scheme 1. Radiosynthesis of [^{11}C]**1**. Reagents and conditions, (a) DIPEA (10 eq), DMPU, 100 °C, 2 min.; Cyclotron irradiation time; 10 min (30 μA); Total synthetic time; 30 min. EOS, end of synthesis.

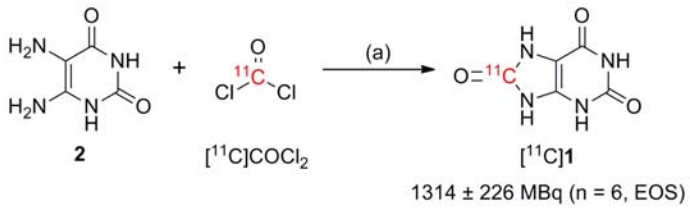

Figure 2. HPLC chromatograms of [^{11}C]**1**. (A): before purification (B): after purification. UV absorbance, 290 nm. UV absorption at around 2 min is caused by solvents present in the injection solution (B).

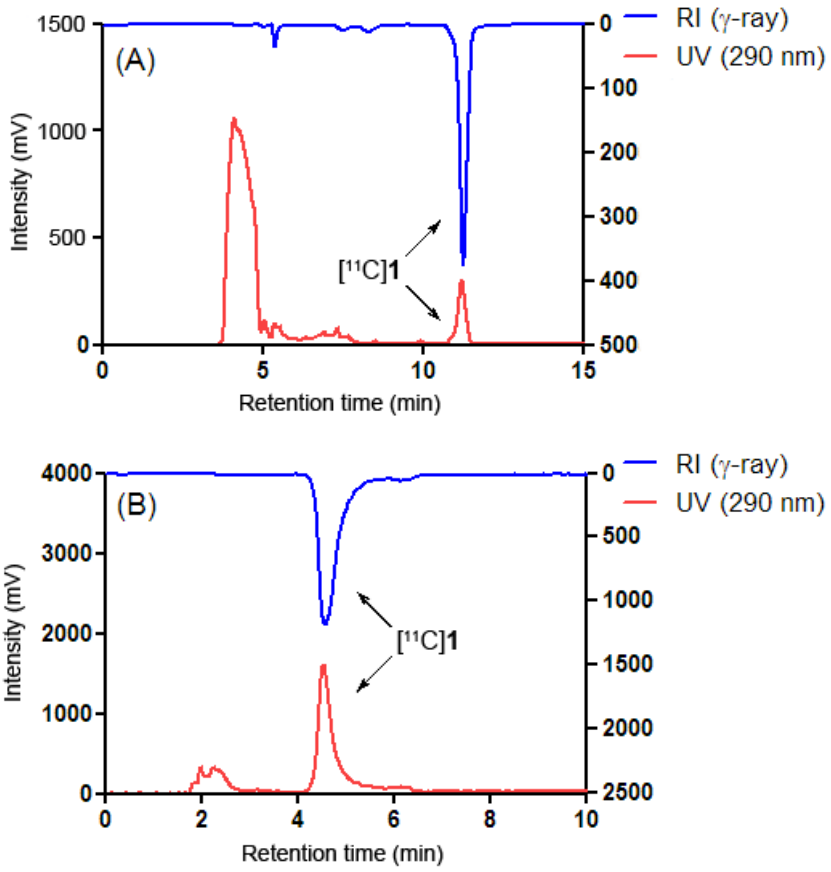

Scheme 2. Synthesis of [^{11}C]**1** from **3**.

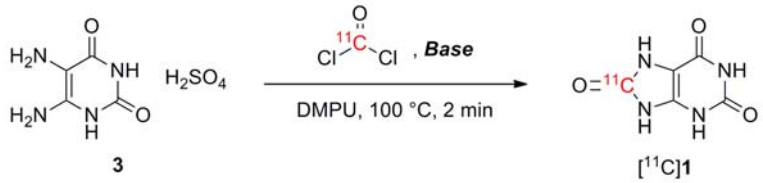

Table 1. Impact of various bases on radiochemical yield of [^{11}C]**1** from **3**.

Entry	***Base***	Additive	Yield (MBq, EOS)
1	NEt_3 (10 eq)		ND
2	DIPEA (10 eq)		ND
3	*t*-BuOK (2 eq)		ND
4	*t*-BuOK (2 eq)	18-crown-6 (3 eq)	ND
5	$KN(SiMe_3)_2$ (2 eq)		ND
6	$KN(SiMe_3)_2$ (2 eq)	18-crown-6 (3 eq)	151 ± 35 (n = 3)
7	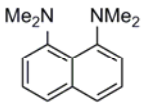 (6 eq)		1231 ± 221 (n = 5)
8	 (6 eq)		1156 ± 198 (n = 3)

Cyclotron irradiation time, 10 min (30 μA); Total synthetic time, 30 min.
EOS, end of synthesis; ND, not detectable.

Figure 3. Representative whole body maximum intensity projection (MIP) image in rats captured at 65-70 min after administration of [^{11}C]**1**. (A: normal condition; B: hyperuricemic condition). Arrows indicate the region of limbs in which higher accumulation of the radioactivity was observed.

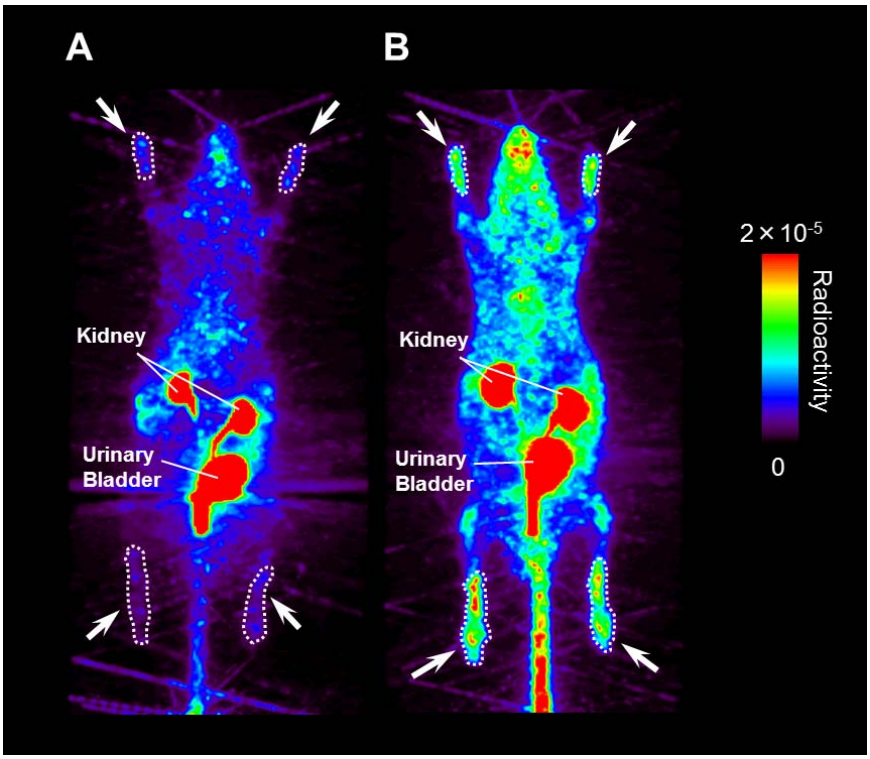

Figure 4. Comparison of (A) radioactivity in limbs at 65-70 min, (B) radioactivity in blood sampled at 60 min, (C) radioactivity remained in the body as determined by subtraction of the radioactivity excreted via renal excretion from that detected in whole body region at 65-70 min following administration of [^{11}C]**1**,and (D) endogenous uric acid level in plasma in rats between normal condition and hyperuricemic condition. Each bar represents the mean ± S.D. (n=3-4 for (A)-(C); n=9 for (D)). The statistically significant differences were observed between control and hyperuricemic condition (Student's unpaired t-test; **, $P < 0.01$, ***, $P < 0.001$)

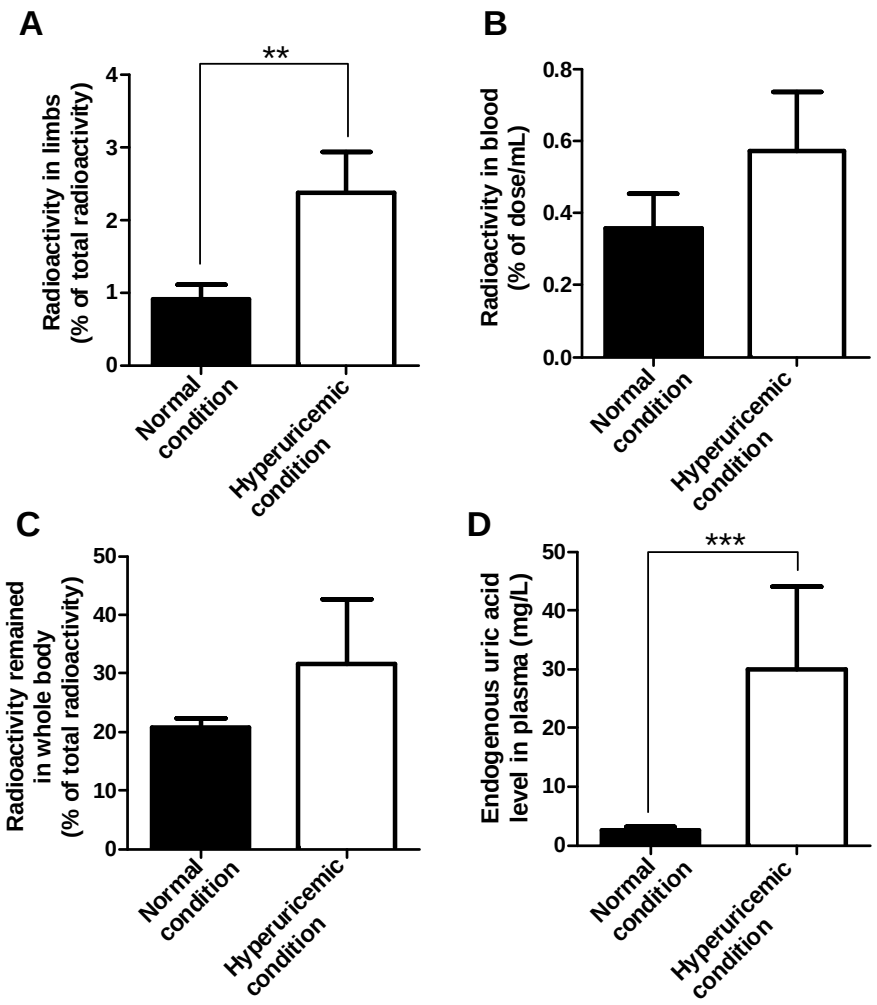
A
**
Radioactivity in limbs
(% of total radioactivity)
4
3
2
1
0
Normal condition
Hyperuricemic condition
B
Radioactivity in blood
(% of dose/mL)
0.8
0.6
0.4
0.2
0.0
Normal condition
Hyperuricemic condition
C
Radioactivity remained
in whole body
(% of total radioactivity)
50
40
30
20
10
0
Normal condition
Hyperuricemic condition
D
***
Endogenous uric acid
level in plasma (mg/L)
50
40
30
20
10
0
Normal condition
Hyperuricemic condition

Figure 5. Representative HPLC radiochromatograms of [^{11}C]**1** and its metabolite in blood specimens. Blood specimens at 30 min of rats under normal condition (A) and hyperuricemic condition (B) were subjected to radiometric HPLC analysis. The identification of the retention time of **1** and hydrophilic metabolite (allantoin) were performed using authentic standard of each compound.